DOI 10.31489/2023PH3/86-90

UDC 535.215; 535.3

C. Bozada

Department of Engineering Physics, Gaziantep University, Turkey
(E-mail: b.ankara@yandex.com)

Effects of Sm doping on EuB_6

A solid-state reaction was used to investigate the nanocrystalline particles of Sm-doped EuB_6 and their optical, thermionic emission and mechanical properties were investigated. The tapered nanoawls had a length of 3–12 μm and a diameter ranging from 40 to 200 nm at the roots and 20–100 nm at the tip as shown by in scanning electron microscopy (SEM). As the temperature of the material increases, the thermionic emission current density also increases. J_o as the zero-field current densities for $Eu_{0.6}Sm_{0.4}B_6$ at 1500 K, 1673 K, 1773 K, 1873 K were 0.72 A cm^{-2}, 4.25 A cm^{-2}, 10.06 A cm^{-2} and 20.05 A cm^{-2}. By increasing the Sm doping content, electrical density of $Eu_{1-x}Sm_xB_6$ decreases. In all materials, the electrical resistivities increased linearly with temperature from 200 to 1200 °C, indicating metallic conductivity. $Eu_{0.6}Sm_{0.4}B_6$ has a lower Vickers hardness and higher flexural strength than EuB_6.

Keywords: nanocrystalline, mechanical properties, dielectric function, thermionic emission, electrical resistivity.

Introduction

Europium hexaboride (EuB_6) is the rare-earth metal hexaboride (REB_6). Among ferromagnetic semiconductors, EuB_6 shows extraordinary magnetoresistance and is commonly believed to include magnetic polarons [1]. The characteristics of EuB_6 include chemical stability, excellent thermal conductivity, high hardness, high melting point, high wear resistance and a low thermal expansion coefficient. Both boron (B) and europium (Eu) atoms exhibit high neutron absorption cross sections, EuB_6 acts as an excellent neutron absorber and is used as a control rod in fast breeder reactor [2].

Samarium hexaboride (SmB_6) is both Kondo insulator(KIs) and heavy fermion semiconductor as well as an exotic material by means of powerful electronic relationships where occupied 4f electrons lead to novel ground states [3]. It is an intermediate-valence compound, that which is a narrow-gap semiconductor [4]. SmB_6 is a very hard and stable rare-earth hexaboride(REB_6). When the temperature is low, SmB_6 becomes ferromagnetic [5]. SmB_6 applications include field emitters, photodetectors, cathodes and energy storage [6].

Bao et al. [7] studied the structure and optical adsorption of the powder of Eu-doped SmB_6 via a solid-state reaction. They reported that the reaction temperature improved the grain size and powder distribution of the synthesized samples. By increasing Eu doping, the transmissivity as a function of the wavelength of SmB_6 increases rectilinear from visible light to near-infrared (NIR). Menth et al. [8] reported that Eu does not significantly change the electrical properties of SmB_6 at low temperatures. SmB_6 exhibits a non-magnetic semiconductor behavior at low temperatures. Yeo et al. [9] investigated the magnetic susceptibilities, resistivities, and Hall effects of Eu-doped SmB_6 ($Sm_{1-x}Eu_xB_6$). EuB_6 is a polaronic ferromagnet and SmB_6 is a Kondo insulator. A narrow f band and broad conduction band hybridize less strongly with Eu doping, and magnetically active ions participate in the AF superexchange interaction as well. Yamaguchi et al. [10] suggested that Eu doping increases the Sm valence and reduces the hybridization of the valence band with Sm 4f. The According to a study Yeo et al. [11], the substitution of Sm for EuB_6 significantly changes its magnetic and transport properties, leading to a transition from ferromagnet to EuB_6 to produce antiferromagnetic and metal-insulator transitions (MITs). The doping of magnetic carriers alters both the itinerant carrier density and magnetic interactions simultaneously.

In this study, nanocrystalline Sm-doped EuB_6 were fabricated via by a solid-state reaction and its optical properties of Sm-doped EuB_6 were investigated. We also investigated their optical properties using first-principle calculations.

Experimental and computational methods

The synthesized nanocrystalline powders were prepared from Eu_2O_3(99.97 %), $SmCl_3 \cdot 6H_2O$ (99.96 %), and $NaBH_4$ (99.98 %). Initially, 600 °C, 800 °C, 1000 °C, and 1200 °C were chosen as the reaction

temperatures for SmB_6 to produce a uniformly distributed nanocrystalline powder. In order to synthesize nanocrystalline Eu-doped SmB_6, the reaction temperature was optimized at 1200 °C. $Sm_{1-x}Eu_xB_6$ powder was examined for phase identification, grain morphology, and microstructure employing field emission scanning electron microscopy(HITACHI SU-8010, FESEM), transmission electron microscopy(TEM, FEI-Tecnai F20 200 kV) and X-ray diffraction (PW1830 with Cu-Kα1 radiation, Philips, XRD).

Sm-doped EuB_6 was analyzed using first-principles calculations based on density-functional theory (DFT) implemented in the VASP computational code [12]. In our calculation, projector augmented wave pseudopotentials with generalized gradient approximation (GGA) and 500 eV kinetic cutoff energy were employed. The surface calculation was sampled using 16×16×1 k-point grids of the Brillouin zone (BZ).

Results and discussion

A graph of the XRD models of $Eu_{1-x}Sm_xB_6$ nanocrystalline powders employed at 1200 °C with x=0, 0.2, 0.4, 0.6, and 0.8 is shown in Figure 1. It appears that the Sm atoms randomly substitute for the Eu atoms in (100), (110), (111), (210), (211), (220), (221), (310), and (222), as indicated by the well-indexed and assigned diffraction peaks. Neither Sm nor Eu peaks were observed in the patterns, indicating that no impurity phase was present in the samples. As can be seen from the patterns, these samples exhibit well-defined peaks, indicating that they were highly crystallized. As shown in Figure 1, all samples consisted of a single phase with a space group of Pm-3m.

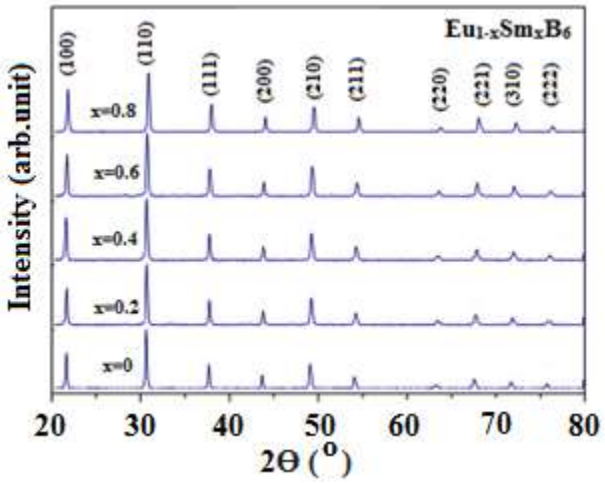

Figure 1. XRD pattern of $Eu_{1-x}Sm_xB_6$ nanopowder prepeared at 1200 °C.

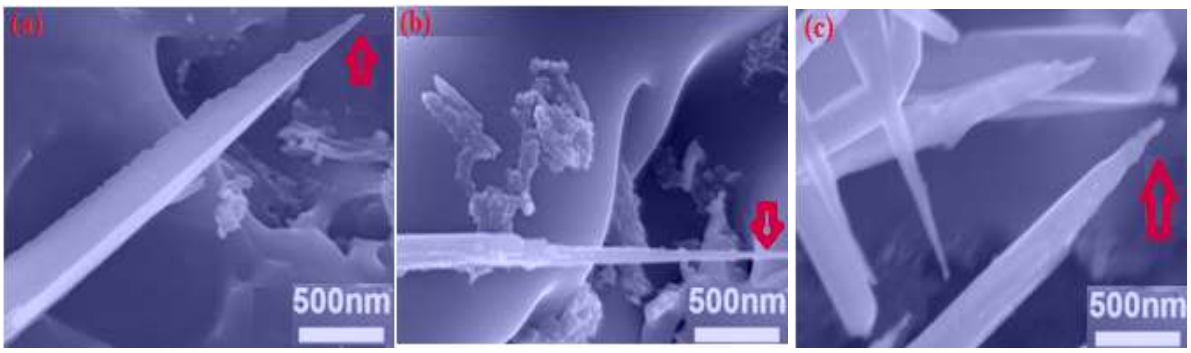

Figure 2. SEM images of the $Eu_{1-x}Sm_xB_6$ nanopowder aquired at 1200 °C

The SEM images of the $Eu_{1-x}Sm_xB_6$ nanopowder were taken at 1200 °C and is depicted in Figure 2. The enlarged images of the $Eu_{1-x}Sm_xB_6$ (x=0.2, 0.4, and 0.6) nanopowders which marked by red arrows with diameters range from approximately 20–100 nm at tip and 40–200 nm at root are presented in Figure 2a-c. In field-induced electron emission, $Eu_{1-x}Sm_xB_6$ are very important and beneficial.

The Vickers hardness, flexural strength, and relative density of $Eu_{0.6}Sm_{0.4}B_6$ were examined at different sintering temperatures. Figure 3 depicts a similar trend, where Vickers hardness, flexural strength, and

relative density gradually increase with temperature until they reach a maximum at 1300 °C. It is considered overfiring when the temperature reaches 1350 C, as evidenced by decrease in the density. Vickers hardness and flexural strength increased with increasing bulk density. The Vickers hardness and flexural strength values have been measured at 1300 °C to be 22.4 GPa, 241 MPa and respectively. EuB_6 has a Vickers hardness and flexural strength of 26.1GPa and 183MPa, respectively [2]. Hence the Vickers hardness of $Eu_{0.6}Sm_{0.4}B_6$ is smaller than EuB_6 and flexural strength of $Eu_{0.6}Sm_{0.4}B_6$ are higher than EuB_6.

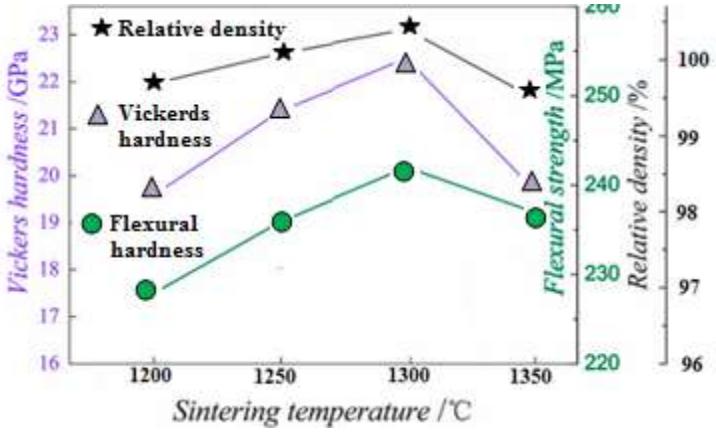

Figure 3. Flexural strength, Vickers hardness, and relative density of $Eu_{0.6}Sm_{0.4}B_6$ at different sintering temperatures.

Figure 4 shows typical Schottky plots (logJ–$U^{1/2}$ curves) for $Eu_{0.6}Sm_{0.4}B_6$. Temperature-limited values are extrapolated back to zero-field theory in the evaluation of the work function. The Richardson–Dushman formula can be written as follows: $Lg(J/T^2) = LgA - 5040\ \phi/T$. A(120 A cm^{-2} K^{-2}) is Richardson's constant, ϕ (eV) is the emitter work function, T (K) is the temperature and J(A cm^{-2}) is the emission current density. The zero field current densities(J_o) of $Eu_{0.6}Sm_{0.4}B_6$ are obtained at 1500K, 1673 K, 1773 K, 1873 K were 0.72 A cm^{-2}, 4.25 A cm^{-2}, 10.06 A cm^{-2} and 20.05 A cm^{-2}, respectively. Thermal emission current density increases as material temperature increases.

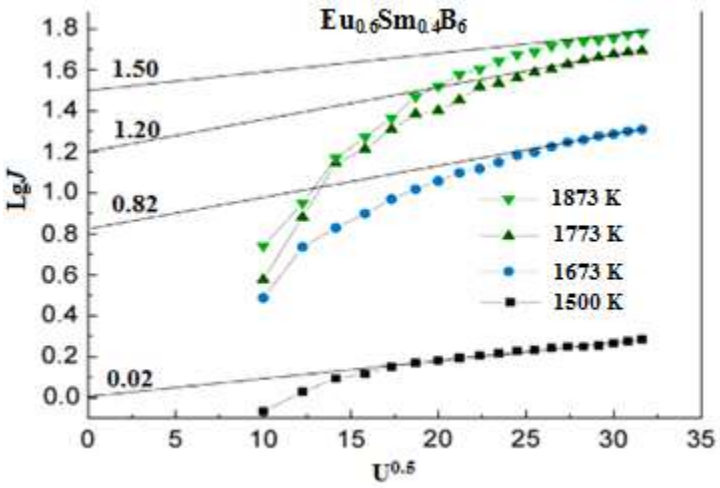

Figure 4. Typical Schottky plots for $Eu_{0.6}Sm_{0.4}B_6$

The UV-VIS absorption spectra of EuB_6 and $Eu_{0.4}Sm_{0.6}B_6$ are shown in Figure 5. The pure EuB_6 and $Eu_{0.4}Sm_{0.6}B_6$ peaks have an absorption shoulder centered at 220 nm. When the absorption peak positions were compared, they were considerably shifted towards the red region. Pure EuB_6 exhibited stronger light absorption at 150 nm than Sm doped with EuB_6.

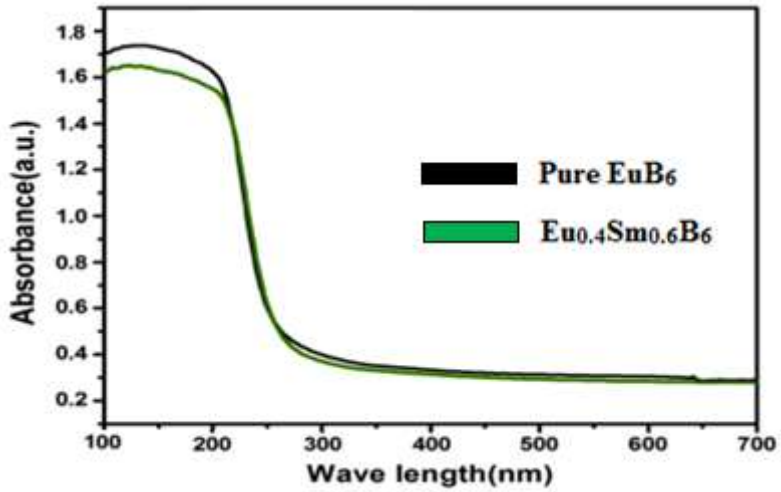

Figure 5. Absorption spectra of pure EuB_6 and $Eu_{0.4}Sm_{0.6}B_6$

The electrical resistivity is shown in Figure 6 as a function of the temperature for different doping contents. Metallic conducting behavior is observed in all samples, as their electrical resistivities increased linearly with temperature from 200 to 1200 °C. Using a 60 % Sm doping content, the electrical resistivity became 4350 Ω cm at 200 °C and 9000 Ω cm at 1200 °C. Additionally, a decrease in the electrical resistivity is also observed when the Sm doping content increases to 80 and 100 at.%, indicating that electrical resistivity is decreased by Sm doping.

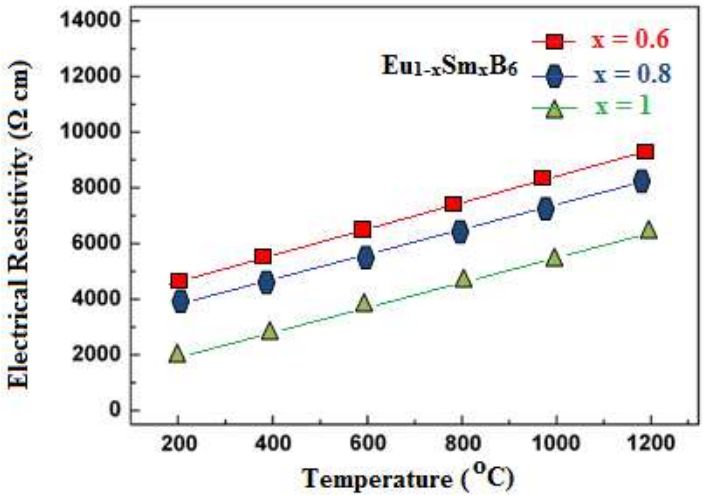

Figure 6. Electric resistivity for $Eu_{1-x}Sm_xB_6$ as a function of temperature.

Conclusions

The Optical, thermoelectric and mechanical properties of Sm-doped EuB_6 nanocrystalline particles were investigated using solid-state reactions. Tapered nanoawls shown by scanning electron microscopy (SEM) have a length of 3–12 μm and a diameter ranging from 40 to 200 nm at the roots and 20–100 nm at the tip. The thermionic emission current density increases with increasing material temperature. Eu0.6Sm0.4B6 had zero field current densities(J_o) of 0.72 A cm^{-2}, 4.25 A cm^{-2}, 10.06 A cm^{-2} and 20.05 A cm^{-2} at 1500 K, 1673 K, 1773 K, and 1873 K, respectively. The electrical density of $Eu_{1-x}Sm_xB_6$ decreases with increasing Sm doping content. In the temperature range of 200 — 1200 °C, the electrical resistivity of all materials increased linearly, indicating that they were metallically conductive. In contrast to EuB_6, $Eu_{0.6}Sm_{0.4}B_6$ has a smaller Vickers hardness and higher flexural strength.

Data Availability

The raw/processed data required to reproduce these findings cannot be shared at this time due to technical or time limitations.

References

1 Sivananda, D. J. & et al. (2018). Stepwise disintegration of magnetic domains in a EuB 6 single crystal observed by magneto-optical imaging.

2 Sonber, J. K., Murthy, T. S. R. C., Subramanian C., Hubli R. C. & Suri A. K.(2013). Synthesis, densification and characterization of EuB6. *Int. J. Refract. Met. Hard Mater., 38*, 67–72.

3 Jiang, J. et al. (2013). Observation of possible topological in-gap surface states in the Kondo insulator SmB6 by photoemission. *Nat. Commun., 4*(1), 1–8.

4 Sluchanko, N. E. et al. (2000). Intragap states in SmB 6. *Phys. Rev. B., 61*(15), 9906.

5 Xiao, L., Su, Y., Peng, P. & Tang, D. (2017). First-principles study of electronic, mechanical and optical properties of mixed valence SmB 6. *IOP Conf. Ser. Mater. Sci. Eng., 207*(1). doi: 10.1088/1757-899X/207/1/012084.

6 Wang, Z. & Han, W. (2021). Recent Developments on Rare-Earth Hexaboride Nanowires, Sustainability, *13*(24), 13970.

7 Bao, L., Ning, J. & Liu, Z. (2021). Mechanism for transmittance light tunable property of nanocrystalline Eu-doped SmB6: Experimental and first-principles study. *J. Rare Earths, 39*(9), 1100–1107.

8 Geballe, T. H., Menth, A., Buehler, E. & Hull, G. W. (1970). Properties of SmB6 doped with Eu and Gd. J. *Appl. Phys., 41*(3), 904–905.

9 Yeo, S., Song, K., Hur, N., Fisk, Z. & Schlottmann, P. (2012). Effects of Eu doping on SmB 6 single crystals. *Phys. Rev. B., 85*(11), 115125.

10 Yamaguchi, J. et al. (2010). Strongly correlated electronic states of Yb1− xLuxB12 and Smi1− yEuyB6 studied by highly bulk-sensitive photoelectron spectroscopy. *Journal of Physics: Conference Series, 200*(1), 12230.

11 Yeo, S.J. Bunder, E., Lin, H.-H., Jung, M.-H. & Lee, S.-I. Concurrent magnetic and metal-insulator transitions in Eu 1− x Sm x B 6 single crystals. *Appl. Phys. Lett., 94*(4), 42509.

12 Hobbs, D., Kresse, G. & Hafner, J. Fully unconstrained noncollinear magnetism within the projector augmented-wave method. *Phys. Rev., B. 62*(17), 11556.

Ч. Бозада

Легирленген Sm-нің EuB_6-ға әсері

Қатты фазалық реакция көмегімен легирленген Sm-нің EuB_6 нанокристалды бөлшектері зерттеліп, олардың оптикалық, термиялық және механикалық қасиеттері зерттелді. Сканерлеуші электронды микроскопияның көмегімен көрсетілгендей, конустық наноқабықшаларының ұзындығы 3-12 мкм және диаметрі тамырларда 40-тан 200 нм-ге дейін және ұшында 20-100 нм-ге дейін болды. Материалдың температурасы көтерілген сайын термоэлектрлі эмиссиялық токтың тығыздығы да артады. 1500 К, 1673 К, 1773 К, 1873 К кезінде $Eu_{0.6}Sm_{0.4}B_6$ үшін Jo нөлдік өріс ток тығыздығы 0,72 А см-2, 4,25 А см-2, 10,06 А см-2 және 20,05 А см-2 құрады. Sm легирленуінің мөлшері артқан сайын Eu1-xSmxB6 электр тығыздығы төмендейді. Барлық материалдарда меншікті электр кедергісі 200-ден 1200 °C-қа дейінгі температурада сызықтық түрде өсті, бұл металл өткізгіштігін көрсетеді. $Eu_{0.6}Sm_{0.4}B_6$ EuB_6. қарағанда Виккерс бойынша қаттылығы төмен және иілу беріктігі жоғары.

Кілт сөздері: нанокристалдар, механикалық қасиеттер, диэлектрлік функция, термоэлектрондық эмиссия, меншікті электр кедергісі.

Ч. Бозада

Влияние легирования Sm на EuB_6

С помощью твердофазной реакции исследованы нанокристаллические частицы EuB_6, легированные Sm, и исследованы их оптические, термоэмиссионные и механические свойства. Как показано, с помощью сканирующей электронной микроскопии конические наностержни имели длину 3–12 мкм и диаметр в диапазоне от 40 до 200 нм у корней и 20–100 нм на кончике. С повышением температуры материала плотность тока термоэлектронной эмиссии также увеличивается. Jo, поскольку плотности тока в нулевом поле для $Eu_{0.6}Sm_{0.4}B_6$ при 1500 К, 1673 К, 1773 К, 1873 К, составляли 0,72 А см-2, 4,25 А см-2, 10,06 А см-2 и 20,05 А см-2. При увеличении содержания легирования Sm электрическая плотность $Eu_{1-x}Sm_xB_6$ снижается. Во всех материалах удельное электрическое сопротивление линейно возрастало с температурой от 200 до 1200°C, что указывает на металлическую проводимость. $Eu_{0.6}Sm_{0.4}B_6$ имеет более низкую твердость по Виккерсу и более высокую прочность на изгиб, чем EuB_6.

Ключевые слова: нанокристаллы, механические свойства, диэлектрическая функция, термоэлектронная эмиссия, удельное электрическое сопротивление.